# Low-Loss Highly Tolerant Flip-Chip Couplers for Hybrid Integration of $Si_3N_4$ and Polymer Waveguides

Jinfeng Mu, Theonitsa Alexoudi, Yean-Sheng Yong, Sergio A. Vázquez-Córdova, Meindert Dijkstra, Kerstin Wörhoff, Jeroen Duis, and Sonia M. García-Blanco, *Member, IEEE*

***Abstract*— In this letter, low-loss and highly fabrication-tolerant flip-chip bonded vertical couplers under single-mode condition are demonstrated for the integration of a polymer waveguide chip onto the $Si_3N_4/SiO_2$ passive platform. The passively aligned vertical couplers have a lateral misalignment between polymer and $Si_3N_4$ waveguide cores of ±1.25 μm. Low-loss operation has been experimentally demonstrated over a wide spectral window of 1480–1560 nm, with measured coupler losses below 0.8 dB for $Si_3N_4$ taper angles below 1.2°, in good agreement with the calculated values. Furthermore, thermal shock test results show less than 0.1 dB degradation, indicating a robust coupling performance.**

***Index Terms*— Vertical coupler, flip-chip bonding, silicon nitride, polymer, hybrid integration.**

## I. Introduction

THE progress of integrated optics increasingly requires the integration of multiple diverse components such as laser sources, detectors, modulators and switches into a single photonic chip. Over the past decade, great effort has been spent on the hybrid integration of the passive silicon-on-insulator (SOI) platform with semiconductor materials such as germanium (Ge) and InP to realize active modulators and lasers [1]. Moreover, due to its ultra-low propagation loss of <1 dB/m in the C-band [2] and large transparency window, i.e. 0.4-2.35 μm [3], the passive $Si_3N_4$ platform integrated with other materials such as polymer [4], InGaAs [5] and rare-earth-ion-doped $Al_2O_3$ [6] has attracted significant interest. Especially the integration with cost-effective polymer materials has led to the demonstration of power-efficient thermally tunable filters [4] and fast modulators [7] (> 100 GHz) due to their electro-optic effect as well as good efficiency for heat insulation.

Manuscript received June 21, 2016; revised August 3, 2016 and September 15, 2016; accepted October 1, 2016. Date of publication October 7, 2016; date of current version November 3, 2016. This work was supported by the Stichting voor de Technisch Wetenschappen (STW) under Project STW-13536.

J. Mu, Y.-S. Yong, S. A. Vázquez-Córdova, M. Dijkstra, and S. M. García-Blanco are with the Optical Sciences Group, MESA+ Institute for Nanotechnology, University of Twente, 7500AE Enschede, The Netherlands (e-mail: j.mu@utwente.nl).

T. Alexoudi is with the Department of Informatics, Aristotle University of Thessaloniki, 54124 Thessaloniki, Greece.

K. Wörhoff is with Lionix B.V., 7500AL Enschede, The Netherlands.

J. Duis is with TE Connectivity Nederland B.V., 5222AR 's-Hertogenbosch, The Netherlands.

Color versions of one or more of the figures in this letter are available online at http://ieeexplore.ieee.org.

Digital Object Identifier 10.1109/LPT.2016.2616021

Still, the low-loss optical coupling between chips remains one of the biggest challenges. Two coupling schemes are generally utilized in hybrid integrated platforms, i.e., the resonant and the adiabatic coupling schemes [8]. The former requires precise determination of the half beat length to achieve optimal coupling efficiency, which is normally very difficult to fabricate with sufficient accuracy. The latter option overcomes this issue by gradually varying the effective refractive index of the propagating mode to obtain high coupling efficiency and higher tolerance to fabrication errors.

In the design of the adiabatic vertical couplers employed in most hybrid integrated SOI chips, the mode mismatch losses caused by the abrupt geometry changes at the taper tips are not considered [9], [10]. The width of the tip of the SOI taper is made to reach the cut-off condition by means of electron-beam or stepper lithography techniques. As a consequence, the SOI taper tip hardly affects the propagating mode in the coupled waveguide system. Additionally, the highly confined mode in the SOI waveguide is less affected at the polymer taper tip. Therefore, the propagation losses of the SOI waveguides dominate over the small mode mismatch loss at both taper tips. In the case of ultra-low loss $Si_3N_4$ waveguides, the mode mismatch play a predominant role in the overall losses of the device and an optimal design is required. This is especially relevant when using contact optical lithography with a relatively large resolution limit (>0.8 μm). Recently, IBM Inc. experimentally demonstrated flip-chip couplers between SOI photonic chips and optical carriers [10], showing high tolerance to a lateral polymer-Si misalignment of ±2 μm. Flip-chip bonding enables the integration of "known-good-dies" without having to develop new fabrication flows for each new material. It can thus reduce the overall cost and development time. Till date, flip-chip coupling between polymer and $Si_3N_4$ chips has not yet been reported.

In this letter, we present the development of low-loss highly tolerant vertical couplers for hybrid integration in $Si_3N_4/SiO_2$ technology. An optimal design of the vertical couplers is obtained by employing an efficient hybrid method, combining the two-dimensional (2D) film mode matching (FMM) method and three-dimensional (3D) eigenmode expansion method (EME). For the demonstration of the developed technology, the epoxy-based negative resist SU-8 is selected to fabricate the polymer waveguides. The polymer chip is then flip-chip bonded onto the stripe $Si_3N_4$ waveguides.

1041-1135 © 2016 IEEE. Personal use is permitted, but republication/redistribution requires IEEE permission.
See http://www.ieee.org/publications_standards/publications/rights/index.html for more information.

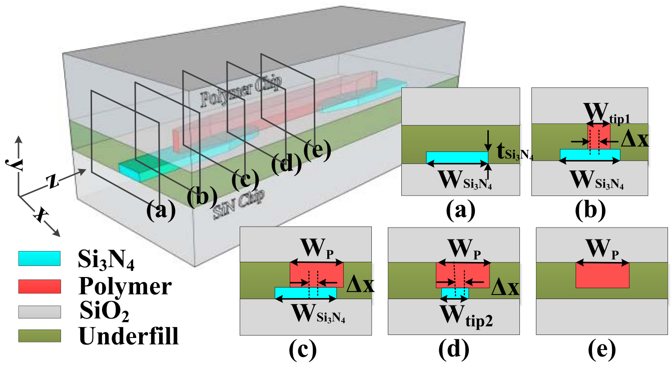


Fig. 1. 3D schematic of vertical coupler with the cross-sections: (a) at $Si_3N_4$ waveguide input/output, (b) at the polymer taper tip, (c) at the start of polymer/$Si_3N_4$ taper, (d) at the $Si_3N_4$ taper tip, and (e) at polymer waveguide input/output.

Successful operation is experimentally verified for the fabricated couplers in the spectral window of 1.48-1.56 $\mu$m both before and after thermal shock tests.

## II. Design of the Vertical Couplers

Fig. 1 shows a 3D schematic of the vertical coupler and the corresponding cross-sections (CS) at different locations along the propagation direction: (a) at the $Si_3N_4$ waveguide input/output, (b) at the tip of the polymer taper, (c) at the start of the polymer/$Si_3N_4$ taper, (d) at the tip of the $Si_3N_4$ taper, (e) at the polymer waveguide input/output. To transfer the electromagnetic field vertically between the $Si_3N_4$ and polymer waveguides, both the $Si_3N_4$ and polymer waveguides are linearly tapered in the coupling region, i.e., between the CS at (b) and (d). The device is designed to work for the transverse-electric (TE) polarization.

The mode mismatch losses between the CS (a) and (b), $\alpha_1$ and between the CS (d), and (e), $\alpha_2$, can be neglected only when the perturbation of the effective refractive index at the taper tip is small enough. The mode mismatch loss expressed in dB can be calculated from the mode overlap coefficient, $\Gamma$, as $-10\ log_{10}\Gamma$. Under the adiabatic condition, most of the power of the mode confined in the $Si_3N_4$ core at the CS (b) will be transferred to the mode confined in the polymer core at the CS (d) without conversion to radiation modes. Therefore, the coupler loss ($\alpha_c$) can be estimated by the sum of $\alpha_1$ and $\alpha_2$ (in dB) if the propagation losses can be considered negligible.

To achieve simultaneously low coupler loss and misalignment tolerance during the flip-chip bonding process, multiple parameters including the dimensions of the $Si_3N_4$ and polymer channel waveguides and tapers, the refractive indices of underfill adhesive and polymer material, number of modes in the coupled waveguide system and the lateral misalignment ($\Delta\ x$) between the $Si_3N_4$ and polymer waveguides need to be optimized. In this work, the optical lithography (EVG620) tool employed has a resolution of 0.8 $\mu$m. Hence, the widths of both $Si_3N_4$ and polymer taper tips are designed to be 0.8 $\mu$m. An UV curable adhesive (NOA 84, Norland Adhesives) is used as underfill material and the epoxy-based negative tone photoresist SU-8 is employed to fabricate the polymer waveguides. The refractive indices of the $SiO_2$, NOA adhesive, SU-8, and the $Si_3N_4$ layers at a wavelength of 1.55 $\mu$m are 1.4491, 1.509, 1.574 and 1.9835 respectively for TE polarization, as determined experimentally (Metricon 2010/M and Woollam M-2000UI).

The optimization of all taper parameters by means of 3D methods such as beam propagation method (BPM) [10] or EME [11] comes at a huge computational cost. To overcome this, the design method presented in [12] is adopted. Firstly, fast mode calculations are carried out based on 2D cross-sections at both the polymer taper tip [CS (b) in Fig. 1] and the $Si_3N_4$ taper tip [CS (d) in Fig. 1] by using the FMM method [13]. The mode mismatch losses for multiple combinations of the 2D dimensional parameters, namely the widths and thicknesses of $Si_3N_4$ and polymer waveguides ($W_{Si_3N_4}$, $t_{Si_3N_4}$, $W_P$ and $t_P$,) are calculated. At both polymer and $Si_3N_4$ taper tips, the smaller the taper tip, the smaller its influence on the variation of the effective refractive index of the mode propagating in the $Si_3N_4$ and polymer waveguide cores, respectively. Fig. 2(a) shows the mode mismatch loss $\alpha_1$ as a function of the width of the $Si_3N_4$ waveguide and the thickness of the polymer taper tip for a $Si_3N_4$ thickness of 90 nm. The lower the thickness of the polymer layer, the lower the mismatch loss $\alpha_1$. The opposite occurs at the tip of the $Si_3N_4$ taper tip, where the lowest mode mismatch loss $\alpha_2$ requires the largest polymer thickness, as shown in Fig. 2(b). In order to achieve high tolerance to the lateral $Si_3N_4$-polymer misalignment, the mode should be designed to be less confined with a large mode diameter. Furthermore, the vertical coupler should operate under single-mode condition, indicated by SM in Fig. 2. Thicknesses for the $Si_3N_4$ and polymer layers of 90 nm and 0.5 $\mu$m are selected based on the above considerations. The calculated coupler total losses are shown in Fig. 2(c). A minimum coupler loss of 0.40 dB is found for polymer and $Si_3N_4$ waveguide widths of ~2.9 $\mu$m and ~2.5 $\mu$m respectively, for which the coupler is under multimode operation. In order for the device to be single mode, the width of the $Si_3N_4$ and polymer waveguides should be below 2.4 $\mu$m and 2.7 $\mu$m respectively. A case in the single-mode region of Fig. 2(c) with $W_{Si_3N_4} = 2\ \mu$m and $W_P = 1.5\ \mu$m is selected, far enough from the multimode condition to leave sufficient room for fabrication errors while keeping the polymer section short to avoid adding propagation losses from the SU-8 waveguide section.

3D structures are then constructed with the selected values of $Si_3N_4$ and polymer thicknesses and widths to perform EME simulations to determine the propagation losses neglected by the 2D FMM method, namely the taper loss due to conversion to radiation modes and reflections at the taper tip cross-sections. A small value of 0.25° is chosen for the polymer taper angle. The $Si_3N_4$ taper angles are varied from 0.1° to 1.8°. Fig. 3 shows the loss of the vertical couplers as a function of $Si_3N_4$ taper angle for different lateral misalignments. When the misalignments are small (e.g. $\Delta x < 1.4\ \mu$m), the coupler losses converge at the $Si_3N_4$ taper angle of 0.1°, which is regarded as the adiabatic angle of the $Si_3N_4$ taper. With the increase of $\Delta x$ above 1 $\mu$m, the coupler losses dramatically

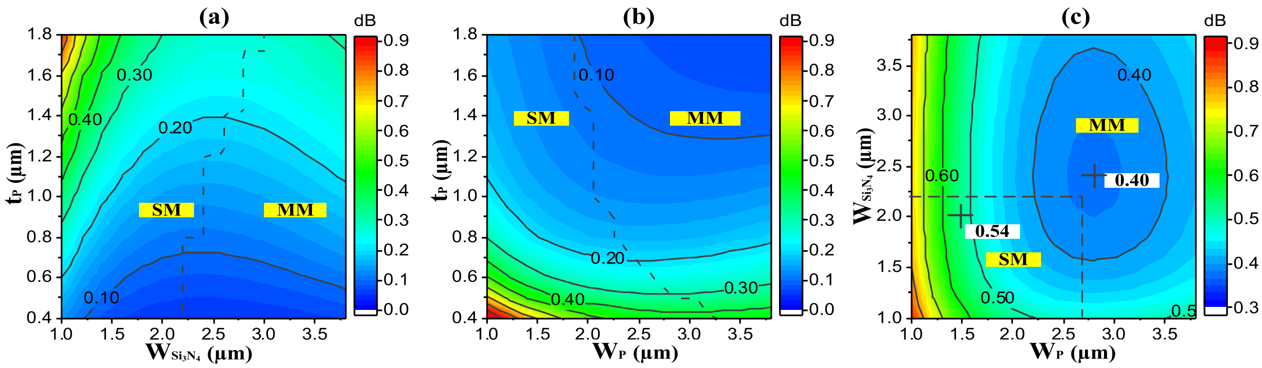

Fig. 2. (a) Mode mismatch loss, $\alpha_1$, at the tip of the polymer taper; (b) mode mismatch loss, $\alpha_2$, at the tip of the $Si_3N_4$ taper, and (c) total loss, $\alpha_c$, for 0.5 $\mu$m thick polymer layer. The tip widths of both polymer and $Si_3N_4$ tapers are 0.8 $\mu$m. The thickness of the $Si_3N_4$ layer is 90 nm. Single-mode (SM) and multimode (MM) conditions of the device are separated by the dashed lines.

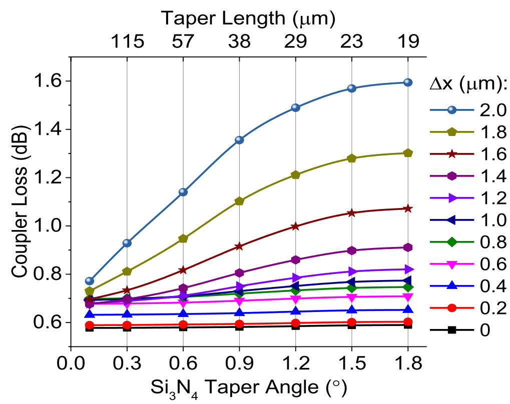

Fig. 3. Coupler losses calculated by EME for different lateral misalignments as a function of $Si_3N_4$ taper angle. The $Si_3N_4$ taper lengths are shown in the top axis. The angle and length of the polymer taper are 0.25° and 80 $\mu$m.

rise and are more significantly affected by the variation of the $Si_3N_4$ taper angle. At the $Si_3N_4$ taper angle of 0.1°, the losses of the couplers without misalignment are 0.57 dB. Additionally, less than 0.9 dB losses can be obtained for couplers with a lateral misalignment range of ±1.4 $\mu$m, which is well within the capabilities of the flip-chip bonder utilized in this work. If higher bonding tolerance is required, smaller $Si_3N_4$ taper angles should be utilized. In order to increase the accuracy of the measurements, waveguides with different numbers of cascaded couplers are fabricated.

Further calculations show that the proposed design works for other polymers with refractive indices ranging between ~1.53 and 1.8. Within this range, a polymer width and thickness can be obtained that keeps the coupler losses below 1 dB while maintaining the single-mode condition for the input and output waveguides and the restriction of a minimum taper tip of 0.8 $\mu$m.

## III. Fabrication Process

The $Si_3N_4$ chip is fabricated by LioniX B.V. [3] based on a single stripe layer geometry, with a fabrication process similar to that described in our recently published work [14] The $Si_3N_4$ layer is deposited on a silicon wafer with a 15 $\mu$m thick thermal oxide using low-pressure chemical vapor deposition (LPCVD). The thickness of the deposited layer is measured to be 92.1 ± 0.6 nm by ellipsometry. In the next step, the $Si_3N_4$ waveguide structures are patterned by contact UV lithography and then etched by reactive ion etching.

To fabricate the polymer waveguides, an SU-8 2000.5 layer is deposited on a borosilicate glass wafer by spin-coating at 3000 rpm (thickness of 0.52 $\mu$m). The SU-8 film is soft-baked for 3 min at 95 °C, and the waveguides are patterned by the same lithography tool. To avoid detachment of the polymer tapers from the substrate, the post-exposure-bake employs multiple steps: 50 °C for 1 min, 65 °C for 1 min, and 80 °C for 3 min with a temperature ramp of 2 °C/min. The unexposed resist is removed with the edge bead remover RER600.

The polymer chip is then flip-chip bonded onto the $Si_3N_4$ waveguides using a flip-chip bonder with a placement accuracy of <1 $\mu$m (Finetech Lambda). The $Si_3N_4$ and polymer waveguides are visually aligned with the aid of a Vernier ruler etched on both chips. Then, the UV curable NOA 84 adhesive is applied on top of the $Si_3N_4$ platform. The bottom stage is heated up to 60 °C to reduce the viscosity of the underfill adhesive. In order to achieve a good contact between the top surfaces of the polymer and the $Si_3N_4$ waveguides without deforming the polymer waveguides, a 10 N bonding force with a ramping speed of 1 N/s is applied. Full curing of the adhesive is achieved by a high-intensity UV curing source (OmniCure 1500) in a nitrogen environment. The bonded chip is then diced to a dimension of 15 mm × 8 mm. Misalignment values of the cascaded vertical couplers ranging from 0.25 $\mu$m to 1.25 $\mu$m are determined from the Vernier scale placed on the chip.

## IV. Experimental Setup and Results

The schematic of the experimental setup is shown in Fig. 4(a). A polarization maintaining (PM) fiber (PM980-XP) was used to couple TE-polarized light from a tunable laser (Agilent 8164B) into the chip. The output is connected to a photodetector by a single-mode fiber (SM-1550). To obtain high-precision alignment, two 3-axes stages (Newport PM-500) are used for the input and output coupling between the waveguide and the fiber. The wavelength used for alignment is 1.55 $\mu$m. A reliability test of the device is performed by thermal shocks consisting of 30 temperature shock cycles from −40 °C to 85 °C according to the standard

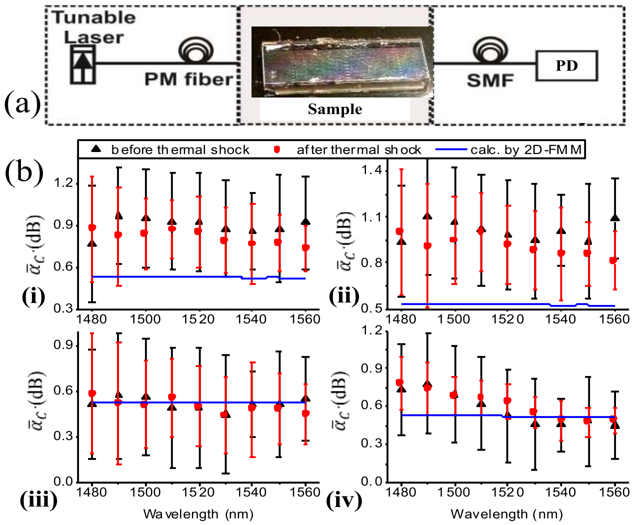


Fig. 4. (a) Experimental setup, and (b) average coupler losses ($\bar{\alpha}_c$) before and after thermal shock tests at different $Si_3N_4$ taper angles and corresponding lengths: (i) 1.8° (19 $\mu$m), (ii) 1.5° (23 $\mu$m), (iii) 1.2° (29 $\mu$m), and (iv) 0.9° (38 $\mu$m). The angle and the length of the polymer taper are 0.25° and 80 $\mu$m.

from the International Electrotechnical Commission (IEC), IEC 60512-11-4: 2002. In each cycle, the chips are kept at the minimum and maximum temperatures for 30 minutes. The chip is characterized both before and after the thermal shock experiment.

The transmission measurements inherently include the wavelength dependent losses from the $Si_3N_4$ waveguide, the polymer waveguide, and the couplers. The propagation loss of the straight $Si_3N_4$ waveguides is <0.1 dB/cm, whereas the loss of the SU-8 waveguides is 3.5-5.5 dB/cm in the spectral window of interest. As the chip is only 1.5 cm long, and the length of polymer straight waveguide connecting one polymer taper to the other is 500 $\mu$m, the measured loss is dominated by the coupling loss of the vertical couplers. A reference straight waveguide without vertical couplers is tested to extract the in-coupling loss of the chip. This figure is assumed to be the same throughout the chip. Hence, the total loss of $N$ cascaded vertical couplers, $\alpha_{c,total}$, can be calculated by subtracting the reference waveguide loss, $\alpha_{ref}$, from the total loss of the waveguide with cascaded couplers, $\alpha_w$. Since each coupler has different misalignment values, the average loss per coupler, $\bar{\alpha}_c = (\alpha_{c,total}/N)$, is utilized as representative performance metric of the fabricated couplers rather than extracting the coupler loss at a specific misalignment.

Fig. 4(b) illustrates the average coupler loss ($\bar{\alpha}_c$) of the fabricated couplers before and after thermal shock tests, as well as the deviation of coupler loss, which includes the uncertainty of the loss measured from the reference waveguides. In the spectral window of interest, the average loss for the couplers with $Si_3N_4$ taper angles between 0.9° and 1.2° is < 0.8 dB, which is in good agreement with the losses calculated from the 2D mode solver, which sets the minimum losses. The couplers with $Si_3N_4$ taper angles of 1.5° and 1.8° are found to have higher losses, probably due to the lower tolerance to misalignment errors shown in Fig. 3. Their losses are still below 1 dB. The couplers with the best performance exhibited losses of ~0.5 dB for all wavelengths in the C-band. Finally, the variation of the average losses per coupler before and after thermal shock is under the measurement uncertainty.

## V. Conclusion

The optimized design of vertical couplers for hybrid integration of $Si_3N_4$ with polymer waveguides based on flip-chip bonding has been presented. Low-loss highly tolerant vertical couplers are designed by using a hybrid method that combines 2D FMM mode solver and 3D EME simulations. The proof-of-concept couplers, working under single-mode condition, are experimentally demonstrated in the spectral window of 1.48-1.56 $\mu$m. Both before and after thermal shock tests (IEC 60512-11-4: 2002), less than 0.8 dB average losses have been measured for all fabricated vertical couplers with measured lateral $Si_3N_4$-polymer misalignments within ±1.25 $\mu$m and $Si_3N_4$ taper angles below 1.2° for all wavelengths in the 1.48-1.56 $\mu$m spectral window. The proposed coupling technology holds the credentials for on-chip-scale integration of the $Si_3N_4$ platform with polymer waveguides.

## References


[1] M. Smit, J. van der Tol, and M. Hill, "Moore's law in photonics," *Laser Photon. Rev.*, vol. 6, no. 1, pp. 1–13, Jan. 2012.

[2] J. F. Bauters *et al.*, "Ultra-low-loss high-aspect-ratio $Si_3N_4$ waveguides," *Opt. Exp.*, vol. 19, pp. 3163–3174, Feb. 2011.

[3] K. Wörhoff, R. G. Heideman, A. Leinse, and M. Hoekman, "TriPleX: A versatile dielectric photonic platform," *Adv. Opt. Technol.*, vol. 4, pp. 189–207, Apr. 2015.

[4] Z. Zhang, G. Genrich, N. Keil, and N. Grote, "Widely tunable grating-assisted heterogeneous silicon nitride/polymer waveguide coupler," *Opt. Lett.*, vol. 39, pp. 162–165, Jan. 2014.

[5] M. Piels, J. F. Bauters, M. L. Davenport, M. J. R. Heck, and J. E. Bowers, "Low-loss silicon nitride AWG demultiplexer heterogeneously integrated with hybrid III–V/silicon photodetectors," *J. Lightw. Technol.*, vol. 32, no. 4, pp. 817–823, Feb. 15, 2014.

[6] J. D. B. Bradley *et al.*, "Monolithic erbium- and ytterbium-doped microring lasers on silicon chips," *Opt. Exp.*, vol. 22, pp. 12226–12237, May 2014.

[7] P. Groumas *et al.*, "Multi-100 GbE and 400 GbE interfaces for intra-data center networks based on arrayed transceivers with serial 100 Gb/s operation," *J. Lightw. Technol.*, vol. 33, no. 4, pp. 943–954, Feb. 15, 2015.

[8] M. Galarza, D. Van Thourhout, R. Baets, and M. Lopez-Amo, "Compact and highly-efficient polarization independent vertical resonant couplers for active-passive monolithic integration," *Opt. Exp.*, vol. 16, pp. 8350–8358, Jun. 2008.

[9] J. Shu, C. Qiu, X. Zhang, and Q. Xu, "Efficient coupler between chip-level and board-level optical waveguides," *Opt. Lett.*, vol. 36, pp. 3614–3616, Sep. 2011.

[10] I. M. Soganci, A. La Porta, and B. J. Offrein, "Flip-chip optical couplers with scalable I/O count for silicon photonics," *Opt. Exp.*, vol. 21, no. 13, pp. 16075–16085, Jul. 2013.

[11] L. Lever, Z. Ikonić, and R. W. Kelsall, "Adiabatic mode coupling between SiGe photonic devices and SOI waveguides," *Opt. Exp.*, vol. 20, pp. 29500–29506, Dec. 2012.

[12] J. Mu, M. A. Sefunc, B. Xu, M. Dijkstra, and S. M. García-Blanco, "Design and fabrication of adiabatic vertical couplers for hybrid integration by flip-chip bonding," *Proc. SPIE*, vol. 9750, pp. 975012-1–975012-10, Mar. 2016.

[13] A. S. Sudbo, "Film mode matching: A versatile numerical method for vector mode field calculations in dielectric waveguides," *Pure Appl. Opt., J. Eur. Opt. Soc. A*, vol. 2, no. 3, p. 211, 1993.

[14] J. Mu, S. Vázquez-Córdova, M. A. Sefunc, Y.-S. Yong, and S. M. García-Blanco, "A low-loss and broadband MMI-based multi/demultiplexer in $Si_3N_4/SiO_2$ technology," *J. Lightw. Technol.*, vol. 34, no. 15, pp. 3603–3609, Aug. 1, 2016.